https://doi.org/10.2352/CIC.2022.30.1.20

Comparison of LED-based and reflective colour targets for camera spectral sensitivities estimation

Hui Fan, Ming Ronnier Luo*
State Key Laboratory of Modern Optical Instrumentation, Zhejiang University, Hangzhou, China
****m.r.luo@zju.edu.cn.***

Abstract

Spectral sensitivities represent the spectral property of a digital camera. Most of the prior art spectral sensitivities estimation algorithms were applied to reflective colour charts, while some algorithms used a LED-based target. In this study, the spectral sensitivities of camera were estimated from both the LED-based and reflective colour targets. Four algorithms including Tikhonov Regularization based on Derivatives, Fourier basis function, Principal Component Analysis (PCA) and Singular Value Decomposition (SVD), were implemented. The estimated accuracy was compared between different types of colour targets, and between different algorithms. It was found that the optimal algorithm was different when using LED-based and reflective colour targets.

1. Introduction

The spectral sensitivities of a camera describe the spectral response characteristics of the camera. It can be applied in many fields, including multispectral imaging, colour constancy, spectral reflectance recovery, light estimation, prefilter design of camera [1-6]. The standard method of calibrating the spectral sensitivities of a camera is to use a monochromator [7, 8]. However, it is a high-cost device and is time-consuming to capture a series of images over the desired range of wavelength.

In the prior art, various studies have focused on the estimation of camera spectral sensitivities. The samples with different media were applied, including reflective colour chart [9-13] and LED-based target [14-17], while a few studies used fluorescence [18], or even a LCD display [19].

The most frequently used targets for camera spectral sensitivities estimation were reflective colour charts, such as Xrite Macbeth ColorChecker and SG chart. The advantage of using a colour chart is that it only needs a single shoot, and it is convenient and portable to use. However, it also suffers from the limited number of colours, thus colour gamuts, based on one type of colorants. It also needs to be applied together with an illumination device, and has risks of damage, fading and distortion. In addition, the spectral reflectance of the physical objects is generally smooth and has low dimensionality, usually can be expressed by 6-8 basis functions. It is ill-posed to estimate the high-dimensional spectral sensitivities from the reflective objects directly [11]. Thus various algorithms have been applied, including Tikhonov regularization [20], metameric blacks methods [9] , basis functions [10], rank-based method [11], multi-scale convolutional neural network [12], *etc*.

Meanwhile, some studies used LED-based targets for spectral sensitivities estimation. DiCarlo *et al* [14] developed an emissive chart based on narrow band LEDs arranged in a grid pattern. A singular value decomposition method was applied. Bartczak *et al* [15] used a 46-channel spectrally tunable LED light source considered to be narrow band lights to estimate camera spectral sensitivities. Yang [16] used a resolution-enhancement algorithm to reconstruct the spectral responsivity of detector by using multicolor LEDs as probing light sources. Walowit *et al* [17] found that an LED device allowed the use of higher-order eigenvectors extracted from the spectral sensitivity database, resulting in a higher estimated accuracy compared with chart-based method. The advantage of using LED-based target is that it contains multiple channels and could have higher dimensionality than a reflective chart. The spectral tunable LED system can produce flexible spectral signals that cover much wider colour gamut than reflective chart.

However, the feasibility and performance of the prior art algorithms for the two types of targets are not clear. How to choose the appropriate algorithm for LED-based and reflective targets has not been well studied.

In this study, the two different targets were applied for the estimation of camera spectral sensitivities, including a muti-channel LED-based target, and a reflective colour chart. Four algorithms were implemented, including Tikhonov Regularization based on Derivatives, Fourier basis function, Principal Component Analysis (PCA) and Singular Value Decomposition (SVD). The accuracy of different estimation algorithms on different colour targets were compared.

2. Background

Assuming the linear response of a camera, the camera response can be expressed by Eq.(1), where $r(\lambda)$ is the spectral reflectance of the object, $e(\lambda)$ is the spectral power distribution (SPD) of the light, and $s_i(\lambda)$ is the spectral sensitivity of the i th channel. $[\lambda_{min}\, \lambda_{min}]$ is the range of the visible light. C is the number of channels in the camera. For a common trichromatic camera, C equals to 3.

$$R_i = \int_{\lambda_{min}}^{\lambda_{max}} r(\lambda)e(\lambda)s_i(\lambda)d\lambda\,, i = 1,2,\dots C \quad (1)$$

By uniformly sampling the spectra in wavelength, for example from 400nm to 700nm at 10nm interval, the above equation can be written using matrix notation as given in Eq.(2), where *R* is the N by C matrix of camera responses, *r* is the N by 31 spectral reflectance of objects, *E* is the 31 by 31 diagonal matrix representing the SPD of light, and *S* is the 31 by C camera spectral sensitivities. N is the number of the objects.

$$\mathrm{R} = \mathrm{rES} \quad (2)$$

Let *L* equals to the product of *r* and *E*, representing the spectral signals received by the camera, then Eq.(2) becomes,

$$\mathrm{R} = \mathrm{LS} \quad (3)$$

Generally, the goal of camera spectral sensitivities estimation is to solve *S* with known camera response *R* and spectral signals *L*. Then *S* can be solved by least square method following Eq.(4) and Eq.(5).

$$min_S\, ||LS - R||^2 \quad (4)$$

$$S = (L^T L)^{-1} L^T R \quad (5)$$

However, simple regression of the above equations can't work well. It is ill-posed to estimate the spectral sensitivities directly due to the low dimensionality of the real world spectral reflectance. This

makes the spectral signals L rank-deficient and the matrix L^TL almost not invertible [11]. The solution from Eq.(5) is not stable and is significantly influenced by the noise in the camera responses.

As a result, some algorithms aim to obtain a more stable solution. Tikhonov Regularization based on Derivatives [20] adds a penalty term to the original least square error as Eq.(6). Then the closed-form solution of S becomes Eq.(7).

$$min_S\ (||LS-R||^2+\gamma\ ||TS||^2)$$

$$T=\begin{bmatrix} 1 & -1 & 0 & 0 & \cdots & \cdots & \cdots & 0 \\ -1 & 2 & -1 & 0 & \cdots & \cdots & \cdots & 0 \\ 0 & -1 & 2 & -1 & \cdots & \cdots & \cdots & 0 \\ \vdots & \vdots & \vdots & \vdots & \ddots & \vdots & \vdots & \vdots \\ 0 & 0 & 0 & 0 & \cdots & -1 & 2 & -1 \\ 0 & 0 & 0 & 0 & \cdots & 0 & -1 & 1 \end{bmatrix} \quad (6)$$

$$S=(L^TL+\boldsymbol{\gamma}T^TT)^{-1}L^TR \quad (7)$$

The penalty term in Eq.(6) is the second derivative of the solution. T is the second derivative operator, and γ is a positive weight of the penalty term. Larger γ means more constraints on the smoothness of the solution. The value of γ can be determined by plotting L-curve with different γ values [21] (the least square error against the penalty term). The 'corner' of L-curve corresponds to the best γ that can decrease both the least square error and the penalty term simultaneously.

Another classical method is to use basis functions to reduce the dimensionality of the spectral sensitivities. The spectral sensitivities can be expressed by Eq.(8), where B is the basis functions and a is the coefficients.

$$\mathrm{S}=\mathrm{Ba} \quad (8)$$

The common basis functions include polynomial, Fourier basis, radial basis, *etc*. By substituting Eq.(8) into Eq.(3), the spectral sensitivities can be solved using a simple pseudo-inverse method [22] as Eq.(9), where '+' is the pseudo-inverse operator.

$$\mathrm{S}=\mathrm{Ba}=\mathrm{B(LB)^{+}R} \quad (9)$$

Jiang *et al* [10] performed principal component analysis (PCA) on the collected spectral sensitivities database of 28 cameras and found the space was two-dimensional. It is accurate and robust to use PCA-based model to recover the spectral sensitivities of camera compared with other basis functions. While in their studies, Fourier basis was the second most accurate method that only worse than PCA-based method. As a result, PCA-based method and Fourier basis were adopted in this study.

Singular Value Decomposition (SVD) is an effective method to estimate the camera spectral sensitivities by capturing the narrow-band LED [14]. The SVD of spectral signal L can be written as

$$L=UDV^T \quad (10)$$

Here U and V are orthonormal matrices and D is a diagonal matrix with all the singular values arranged on its diagonal in descending order. Suppose the diagonal elements of D is $d_{i,i}$. Combining with pseudo-inverse method, spectral sensitivities can be estimated by Eq.(11). α is a tolerant constant ranged from 0 to 1 defined by the user. The small singular values (less than $\alpha d_{1,1}$) are neglected.

$$\mathrm{S}=\mathrm{V}D'U^TR$$

$$D'=\begin{cases} 1/d_{i,i} & for\ d_{i,i}/d_{1,1}>\alpha \\ 0 & otherwise \end{cases} \quad (11)$$

Due to the independence between the different LED channels, the singular values of the spectral signals decrease slowly so that the spectral sensitivities can be estimated with more degree of freedom. While for a physical reflective chart, the singular values decrease too rapidly due to the correlation between different colour patches [14].

In this study, the above four algorithms were implemented to estimate the camera spectral sensitivities. They are: Tikhonov Regularization based on Derivatives, Fourier basis function, PCA and SVD. These algorithms are all representative methods to estimate the camera spectral sensitivities. The first three methods have been applied by Darrodi *et al* [8, 23] using reflective colour chart as the samples and were proved to be effective. While SVD is suitable to be applied to narrow band LED-based targets. As a result, in this study, the above four algorithms were implemented, and the colour targets of two different media (LED-based and reflective colour charts) were applied and compared.

3. Experiments and Results

Experiments

In this study, LED-based target and reflective colour chart were captured and used for spectral sensitivities estimation, respectively. The LED-based target was a Thouslite® 18-channel spectrum tunable LED system. Figure 1 shows the hardware of the device. The light from LED cube placed on the bottom was reflected and finally emitted horizontally from the circular aperture. Figure 2 shows the normalized SPD of the 18 LED channels.

The tested cameras were a Digital Single Lens Reflex (DSLR) Canon 650D and a mobile camera, the main camera of Huawei P40 Pro. The two cameras were denoted as Camera 1 (DSLR) and Camera 2 (mobile camera), respectively. The ground truth spectral sensitivities of the two cameras were calibrated by a Labsphere QES1000 monochromator.

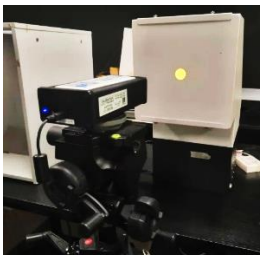

Figure 1. *The hardware of the 18-channel spectrum tunable LED system.*

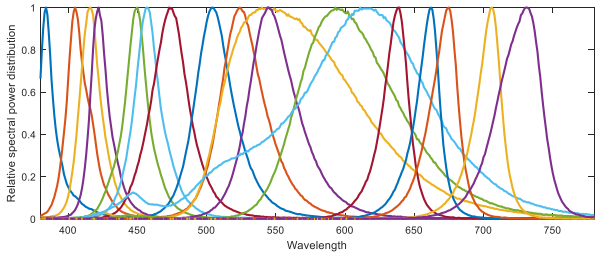

Figure 2. *The normalized SPD of the 18 channels in the LED system.*

The experimental procedure was described as follows. Firstly, use the camera to capture the images of each LED channel at the light emitting plane. The whole measuring process was conducted in a dark room. The position of the camera was adjusted so that the principal axis of the lens was aligned perpendicular to the light emitting plane, and the circular light source was located in the center of the image. The setup of the camera (ISO, shutter speed, F-number, focal length, *etc*) was kept the same throughout the measurement.

The luminance of each LED channel could be adjusted by a given driver value from 0 to 1000. It was adjusted so that when capturing each LED channel, the maximum of R, G and B responses was always about 80%~90% of the saturated response, in order to achieve high signal to noise ratio (SNR). The driver values were recorded. After capturing the images of each LED channel, the LED cubes were turned off, and the image in a completely dark condition was captured to subtract the dark noise from the camera responses. An open-source software 'dcraw' was utilized to obtain the pure RAW images without white balance and other image processing. The camera responses were extracted from the RAW images and were averaged within a square area from the circle. Figure 3 shows an example of the captured image of one of the LED channels and the selected square area.

Then the spectral power distribution (SPD) of each LED channel was measured using a JETI-Specbos 1211 spectroradiometer. The spectroradiometer was placed in the same place as the camera. The intensity of each LED channel was set to the same level as that captured by the camera according to the recorded driver values.

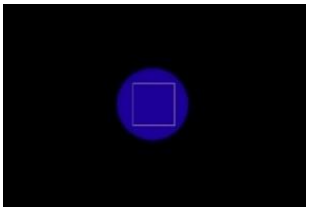

Figure 3. *Example of the image of one LED channel captured by the camera and the selected square area to extract camera responses.*

The reflective colour chart target was an Xrite Macbeth ColorChecker chart (MCCC). It was placed in a Thouslite LED viewing cabinet with an angle of 45° to the horizontal plane. Figure 4 shows the experimental situation. The camera was used to capture the chart, with an illumination/viewing geometry of 45°:0°. A grey board was also captured for the correction of illumination uniformity [24]. The camera responses were extracted from the RAW images. The SPD of the light was measured using a JETI-Specbos 1211 spectroradiometer together with a white plate placed on the center of the bottom of the cabinet. The spectral reflectance of the colour patches was measured using a Datacolor SF600 spectrophotometer, with specular excluded condition. The product of the SPD of light and the spectral reflectance of the patches was considered as the spectral signal L reflected by the colour chart.

The illuminants were simulated D50, D65, and A. Note that the data under D65 were used for spectral sensitivities estimation, while the data under D50 and A were used to test the accuracy of estimated spectral sensitivities in the following sections.

Figure 4. *The experimental situation of capturing MCCC in the LED viewing cabinet.*

Error Metrics

Four error metrics were used to evaluate the accuracy of the estimated spectral sensitivities. They are spectral error, RGB error, CIEDE2000 colour difference (ΔE_{00}), and Vora value. These metrics were also used in the study of Finlayson *et al* [11]. The prevailing metrics in [25] could also be used in the future study. The spectral sensitivities calibrated by the monochromator is considered as the ground truth. The estimated and the ground truth spectral sensitivities are marked as $\hat{S}$ and S, respectively. The spectral error (SE) can be calculated as Eq.(12), indicating the similarity between the shape of $\hat{S}$ and S.

$$\mathrm{SE} = \frac{||\hat{S}-S||}{||S||} \times 100\% \tag{12}$$

The percentage error between the predicted RGB by spectral sensitivities and the measured RGB can represent the accuracy of spectral sensitivities. The predicted RGB is calculated by Eq.(2). Let $\widehat{X}_i$ and X_i donate the predicted and measured camera responses of the sample i. The percentage RGB error can be calculated by Eq.(13), where N is the number of the testing samples. In this study, the testing samples were the 24 colours on MCCC.

$$\Delta \mathrm{X}\% = \frac{1}{N}\sum_{i=1}^{N} \frac{|\widehat{X}_i - X_i|}{|X_i|} \times 100\% \text{ , X=R,G,B} \tag{13}$$

A linear colour correction matrix (CCM) was calculated between the measured RGB and CIE tristimulus values XYZ of the MCCC samples under D50 and A, respectively. The same CCM was then applied to both the predicted RGB by the estimated spectral sensitivities and the measured RGB, and then transformed to CIE L*a*b*. The colour difference ΔE_{00} between them was calculated as an error metric.

Vora value [26] measures the similarity between the vector spaces spanned by the two spectral sensitivities. It is calculated between the estimated and the ground truth spectral sensitivities as defined in Eq.(14). Vora value ranges between 0 and 1. Larger Vora value means that the estimated spectral sensitivities are closer to the ground truth.

$$\mathrm{Vora} = \frac{1}{3} trace\left(S(S^T S)^{-1} S^T \hat{S}\left(\hat{S}^T \hat{S}\right)^{-1} \hat{S}^T\right) \tag{14}$$

Results

The linearity of the camera response was verified by the six neutral patches on the MCCC under D65. It was found that for both cameras, the relationship between camera response and reflectance could be fitted by a linear proportional function with a correlation coefficient greater than 0.999. As a result, no further linearization was conducted. Then the spectral sensitivities of the two cameras (DSLR and mobile camera) were estimated following the four algorithm (Tikhonov Regularization based on Derivatives, Fourier basis function, PCA and SVD) using LED-based target and reflective colour chart, respectively. The LED-based target was the 18 channels of the LED system, and the reflective colour chart was MCCC under D65. The error metrics SE and Vora were calculated comparing with the results of monochromator. The RGB error and ΔE_{00} were calculated using the captured MCCC under D50 and A.

In the Fourier basis method, the different orders of the Fourier basis were attempted and the optimal order was determined with the minimized SE of the estimated spectral sensitivities. It was found that for both cameras, the optimal order of Fourier basis is 8 and 6 when using LED-based and reflective colour chart targets, respectively. The optimal order of Fourier basis was used.

Figures 5 and 6 show the results of the estimated spectral sensitivities following the four algorithms, and the results were compared with those calibrated by the monochromator. Figure 5 is

the results of DSRL (Camera 1) and Figure 6 is of mobile camera (Camera 2). Tables 1 and 2 list the accuracy of the four estimated spectral sensitivities in terms of different metrics. The best result of each metric was marked in bold.

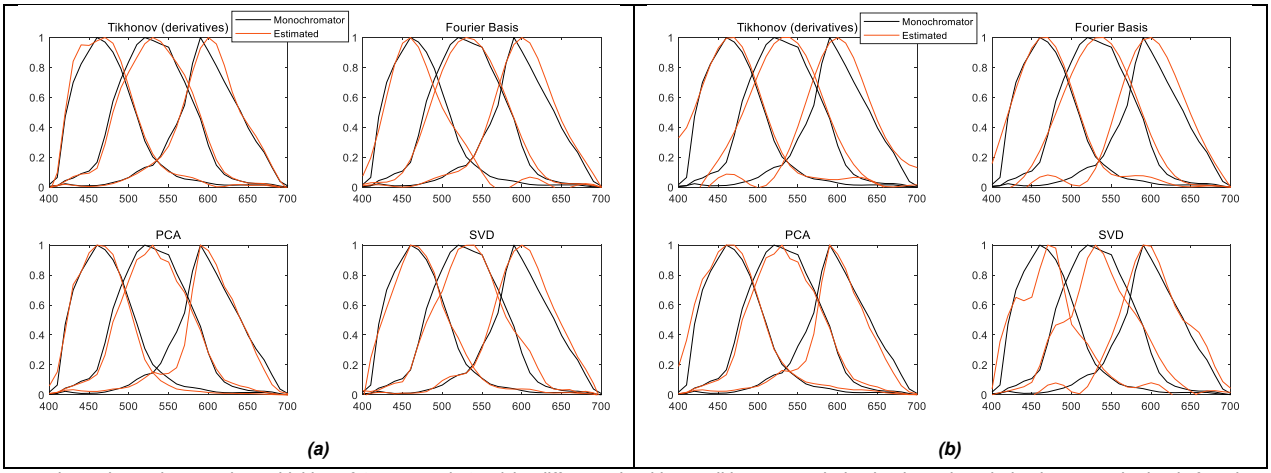

Figure 5. *The estimated spectral sensitivities of Camera 1 (DSLR) by different algorithms: Tikhonov regularization based on derivatives, Fourier basis function, PCA and SVD, and estimated from different media (a) LED-based target, (b) reflective colour chart MCCC.*

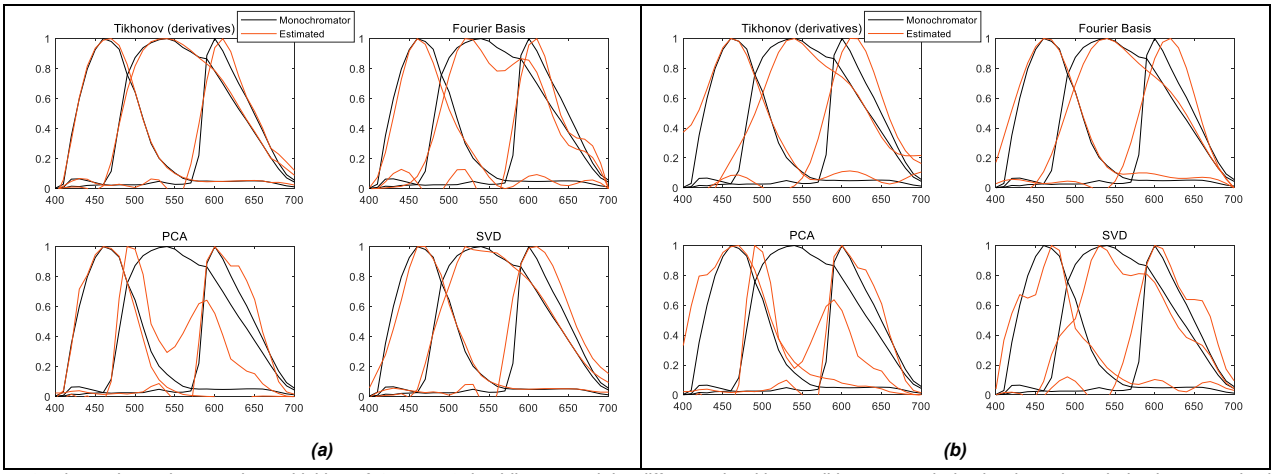

Figure 6. *The estimated spectral sensitivities of Camera 2 (mobile camera) by different algorithms: Tikhonov regularization based on derivatives, Fourier basis function, PCA and SVD, and estimated from different media (a) LED-based target, (b) reflective colour chart MCCC.*

Table 1. The accuracy of estimated spectral sensitivities of Camera 1 (DSLR) in terms of spectral error (SE), RGB error, ΔE_{00}, and Vora value.

LED-based					MCCC				
	Tikhonov (derivatives)	Fourier Basis	PCA	SVD		Tikhonov (derivatives)	Fourier Basis	PCA	SVD
SE(R)	**10.5%**	13.8%	18.3%	14.1%	SE(R)	23.6%	22.4%	**14.8%**	16.0%
SE(G)	**6.9%**	7.3%	7.8%	11.4%	SE(G)	13.6%	9.4%	**7.0%**	19.7%
SE(B)	9.1%	13.0%	**7.7%**	10.9%	SE(B)	19.3%	**12.4%**	15.3%	20.9%
SE mean	**8.8%**	11.4%	11.3%	12.1%	SE mean	18.8%	14.7%	**12.4%**	18.9%
Δ R%	1.00%	0.98%	1.96%	**0.96%**	Δ R%	**1.01%**	1.02%	1.26%	1.14%
Δ G%	**1.21%**	1.23%	1.41%	2.09%	Δ G%	1.30%	**1.20%**	1.48%	1.87%
Δ B%	2.08%	1.69%	6.09%	**1.63%**	Δ B%	2.37%	**1.67%**	2.63%	2.80%
Δ RGB% mean	1.43%	**1.30%**	3.16%	1.56%	Δ RGB% mean	1.56%	**1.30%**	1.79%	1.94%
ΔE_{00}	0.87	**0.73**	2.01	1.05	ΔE_{00}	0.82	**0.66**	0.99	1.06
Vora	**0.994**	0.990	0.990	0.988	Vora	0.966	0.984	**0.985**	0.965

Table 2. The accuracy of estimated spectral sensitivities of Camera 2 (mobile camera) in terms of spectral error (SE), RGB error, ΔE_{00}, and Vora value.

LED-based					MCCC				
	Tikhonov (derivatives)	Fourier Basis	PCA	SVD		Tikhonov (derivatives)	Fourier Basis	PCA	SVD
SE(R)	**17.0%**	22.3%	18.1%	30.3%	SE(R)	30.5%	28.5%	**16.0%**	35.6%
SE(G)	**5.0%**	12.7%	48.7%	7.8%	SE(G)	18.9%	**11.1%**	54.9%	18.6%
SE(B)	**4.4%**	11.6%	11.8%	11.8%	SE(B)	24.1%	**17.0%**	34.1%	23.4%
SE mean	**8.8%**	15.5%	26.2%	16.6%	SE mean	24.5%	**18.9%**	35.0%	25.9%
Δ R%	2.33%	2.53%	3.26%	**2.16%**	Δ R%	**1.99%**	2.30%	2.39%	2.10%
Δ G%	**1.72%**	1.84%	7.59%	1.73%	Δ G%	**1.83%**	2.04%	6.38%	2.07%
Δ B%	3.72%	3.18%	17.63%	**3.08%**	Δ B%	3.40%	**3.11%**	4.80%	3.65%
Δ RGB% mean	2.59%	2.52%	9.50%	**2.32%**	Δ RGB% mean	**2.41%**	2.48%	4.52%	2.60%
ΔE_{00}	1.50	**1.37**	6.51	1.43	ΔE_{00}	0.97	**0.95**	4.20	1.22
Vora	**0.986**	0.974	0.907	0.967	Vora	0.933	**0.955**	0.817	0.924

It was found that Tikhonov regularization based on derivatives significantly outperformed other three methods when using LED-based samples for both cameras. It had the smallest SE and the largest Vora value, proving that the estimated spectral sensitivities by this method had a close match compared with the results calibrated by the monochromator. It could also be verified by directly comparing the estimated and the ground truth spectral sensitivities in Figures 5(a) and 6(a), especially for the results of the mobile camera in Figure 6(a).

When reflective chart MCCC was used as the samples, for all the four algorithms and both cameras, SE increased and Vora value decreased compared with LED-based target. This implied that the estimated spectral sensitivities from LED-based target were more accurate than those from MCCC. The LED-based target in this study was the 18 channels of the LED cube. Most of the LED channels were narrow band and were independent from each other. It could cover large colour gamut close to the spectral locus, as plotted in Figure 7, while the reflective chart covered relatively smaller colour gamut. The samples with wider colorimetric distribution contributed to the better fitting of the spectral sensitivities, especially for the Tikhonov Regularization method. Moreover, the spectral reflectance of the real world objects was smooth and usually had low dimensionality. We performed PCA on the 24 reflectance of MCCC and found that the reflectance could be expressed by at least 7 eigenvectors with mean predicted RMSE error less than 0.01. So it is more challenging to recover the spectral sensitivities from the low-dimensional reflective colour charts than using independent LED channels.

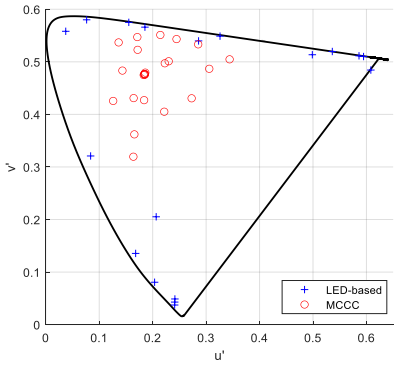

Figure 7. *The chromaticity of the LED-based target and MCCC under D65 in CIE 1976 u'v' plane.*

The PCA method used only the first two eigenvectors obtained from the spectral sensitivities database, so that it could greatly decreased the dimensionality of the unknown spectral sensitivities. This could lead to that, for the DSLR (Camera 1), using LED-based or reflective chart didn't cause significant difference to the accuracy of the estimated spectral sensitivities. The reflective colour chart, although might be low-dimensional, was still sufficient to be used to recover the two-dimensional spectral sensitivities. It seemed that for the DSLR, PCA was the best among the four algorithms when using MCCC as the target, corresponding to the smallest SE and largest Vora value. However, PCA method could only work well for the traditional trichromatic cameras, which was limited by the current spectral sensitivities database. The mobile camera in this study had an unusual broadband G channel thus PCA method failed to recover its spectral sensitivity. The same problem occurred for the Sigma camera in [8].

For the SVD method, as described before, due to the independence between the different LED channels, the singular values of the spectral signals decrease more slowly compared with reflective chart, more non-zero singular values were maintained in Eq.(11), so that the spectral sensitivities can be estimated with more degree of freedom. It can be seen from Tables 1 and 2 that the accuracy of SVD was much lower in terms of SE and Vora value when using MCCC target than using LED-based target. From Figure 5(b) and 6(b), it can also be found that plenty of fluctuation existed in the results of SVD method. So it was not recommended to apply SVD method when using reflective colour chart targets.

It can be noticed from Figures 5 and 6 that the results of Fourier basis method had some high-frequency components in the near-zero region. But this method has stable performance in terms of all the four metrics and using both targets. And it was the optimal method for the mobile camera when using MCCC target.

The RGB error and ΔE_{00} of MCCC were tolerant metrics in this study. The values didn't change significantly for different algorithms (except the failure of PCA for the mobile camera). This could because, the RGB responses were calculated by integrating the spectral sensitivities and spectral signal over wavelength. The values could be similar after integration although errors exist in the estimated spectral sensitivities.

The present results verified that using LED-based target to estimate camera spectral sensitivities led to more accurate results compared with using reflective colour chart. However, the reflective colour chart had the advantages of being convenient to use and manufacture. Applying appropriate algorithms for reflective colour

chart could also achieve acceptable estimated accuracy. In fact, both LED-based and reflective colour targets have their pros and cons. So choosing LED-based or reflective colour chart depends on the actual demand and the available device. In the future, it is worthwhile to further study the factors that can influence the accuracy of spectral sensitivities estimation using different algorithms, including the selection of optimal samples, the number of the samples and the optimized light for the reflective colour chart.

5. Conclusions

In this study, the spectral sensitivities of two cameras (a DSLR and a mobile camera) were estimated by implementing the four algorithms (Tikhonov Regularization based on Derivatives, Fourier basis function, PCA and SVD) using LED-based target and reflective colour chart, respectively. The LED-based target was a muti-channel LED cube, while the reflective colour chart was MCCC under D65. The results showed that the LED-based target could be used to estimate camera spectral sensitivities more accurately than using a reflective colour chart. Meanwhile the colour chart had the advantage of convenient and portable, and also acceptable accuracy when the optimal algorithm was applied. It was found that Tikhonov Regularization based on derivatives outperformed other three methods when using LED-based targets. PCA method had advantages in estimating the spectral sensitivities of common trichromatic cameras from a reflective colour chart. For a camera with uncommon shape of spectral sensitivities and using reflective chart as the target, the method of Fourier basis could work well.

References

[1] J.-I. Park, M.-H. Lee, M. D. Grossberg, and S. K. Nayar, "Multispectral Imaging Using Multiplexed Illumination," in *Proceedings of IEEE International Conference on Computer Vision*, 2007.

[2] G. D. Finlayson and S. D. Hordley, "Color constancy at a pixel," *Journal of the Optical Society of America. A, Optics and image science*, vol. 18, no. 2, pp. 253-264, 2001.

[3] J. X. Liang, K. D. Xiao, and X. R. Hu, "Investigation of light source effects on digital camera-based spectral estimation," *Optics Express*, vol. 29, no. 26, pp. 43899-43916, 2021.

[4] J. Fang, F. Zhang, H. Xu, Z. Wang, and C. Diao, "Spectral estimation of tunable LED light source using digital camera based on matrix factorization," *Optik*, vol. 148, pp. 90-94, 2017.

[5] Y. T. Zhu and G. D. Finlayson, "A Mathematical Investigation into the Design of Prefilters That Make Cameras More Colorimetric dagger," *Sensors*, vol. 20, no. 23, 2020.

[6] E. Walowit and L. Tahoe, "Best Practices for Production Line Camera Color Calibration," 2019.

[7] P. L. Vora, J. E. Farrell, J. D. Tietz, and D. H. Brainard, "Digital Color Cameras - 2 - Spectral Response," 1997.

[8] M. M. Darrodi, G. Finlayson, T. Goodman, and M. Mackiewicz, "Reference data set for camera spectral sensitivity estimation," *Journal of the Optical Society of America a-Optics Image Science and Vision*, vol. 32, no. 3, pp. 381-391, 2015.

[9] A. Alsam and R. Lenz, "Calibrating color cameras using metameric blacks," *Journal of the Optical Society of America a-Optics Image Science and Vision*, vol. 24, no. 1, pp. 11-17, 2007.

[10] J. Jiang, D. Liu, J. Gu, and S. Susstrunk, "What is the space of spectral sensitivity functions for digital color cameras?," in *IEEE Workshop on the Applications of Computer Vision*, 2013, pp. 168-179.

[11] G. Finlayson, M. M. Darrodi, and M. Mackiewicz, "Rank-based camera spectral sensitivity estimation," *J Opt Soc Am A Opt Image Sci Vis*, vol. 33, no. 4, pp. 589-99, 2016.

[12] M. Zhou, W. Chen, T. He, Q. Zhang, and J. Shen, "Scan-free end-to-end new approach for snapshot camera spectral sensitivity estimation," *Opt Lett*, vol. 46, no. 23, pp. 5806-5809, 2021.

[13] Y. Ji, Y. Kwak, S. M. Park, and Y. L. Kim, "Compressive recovery of smartphone RGB spectral sensitivity functions," *Opt Express*, vol. 29, no. 8, pp. 11947-11961, 2021.

[14] J. M. DiCarlo, G. E. Montgomery, and S. W. Trovinger, "Emissive chart for imager calibration," in *12th color and imaging conference*, 2004, pp. 295-301.

[15] P. Bartczak, A. Gebejes, P. Falt, J. Parkkinen, and P. Silfstein, "Led-based spectrally tunable light source for camera characterization," in *Colour and Visual Computing Symposium (CVCS)*, 2015, pp. 1-5.

[16] P.-K. Yang, "Determining the spectral responsivity from relative measurements by using multicolor light-emitting diodes as probing light sources," *Optik*, vol. 126, no. 21, pp. 3088-3092, 2015.

[17] E. Walowit, H. Buhr, and D. Wüller, "Multidimensional Estimation of Spectral Sensitivities," in Colour Imaging Conference, 2017.

[18] S. Han, Y. Matsushita, I. Sato, T. Okabe, and Y. Sato, "Camera spectral sensitivity estimation from a single image under unknown illumination by using fluorescence," in *Proceedings of IEEE Conference on Computer Vision and Pattern Recognition (CVPR)*, 2012, pp. 805-812.

[19] J. Zhu, X. Xie, N. Liao, Z. Zhang, W. Wu, and L. Lv, "Spectral sensitivity estimation of trichromatic camera based on orthogonal test and window filtering," *Opt Express*, vol. 28, no. 19, pp. 28085-28100, 2020.

[20] B. Dyas, "Robust color sensor response characterization," in *Proceedings of Eighth Colour Imaging Conference*, 2000, pp. 144-148.

[21] P. C. Hansen and D. P. O'Leary, "The Use of the L-Curve in the Regularization of Discrete Ill-Posed Problems," *SIAM journal on scientific computing*, vol. 14, no. 6, pp. 1487-1503, 1993.

[22] R. Penrose, "A generalized inverse for matrices," *Mathematical proceedings of the Cambridge Philosophical Society*, vol. 51, no. 3, pp. 406-413, 1955.

[23] M. M. Darrodi, G. Finlayson, T. Goodman, and M. Mackiewicz, "A ground truth data set for Nikon camera's spectral sensitivity estimation," in *Colour Imaging Conference*, 2014, pp. 85-90.

[24] J. Liang, X. Wan, Q. Liu, C. Li, and J. Li, "Research on filter selection method for broadband spectral imaging system based on ancient murals," *Color Research & Application*, vol. 41, no. 6, pp. 585-595, 2016.

[25] J. Hardeberg, "Acquisition and Reproduction of Colour Images: Colorimetric and Multispectral Approaches," 2001.

[26] P. L. Vora and H. J. Trussell, "Mathematical methods for the design of color scanning filters," *IEEE transactions on image processing*, vol. 6, no. 2, pp. 312-320, 1997.

Author Biography

Hui Fan received her BS in Optical Engineering from Nankai University (2020) and she is now a PhD student supervised by Professor Ming Ronnier Luo at Zhejiang University. Her research work is on camera spectral calibration and multispectral imaging.